STRUCTURAL PROPERTIES OF AMORPHOUS RIBBONS PREPARED WITH DIFFERENT VELOCITIES OF THE QUENCHING WHEEL

Narges Amini[1,2], Július Dekan[1], Patrik Novák[1], Safdar Habibi[2] and Marcel Miglierini[1,3]

[1] Institute of Nuclear and Physical Engineering, Slovak University of Technology, Bratislava, Slovakia, [2] Department of Physics, Bu-Ali Sina University, Hamedan, Iran, [3] Department of Nuclear Reactors, Czech Technical University in Prague, Czech Republic.

E-mail: phn.amini@basu.ac.ir

Received 28 April 2016; accepted 13 May 2016

1. Introduction

Iron-based metallic glasses (MGs) have been widely studied during several decades since they not only exhibit excellent soft magnetic properties coupled with good mechanical properties but also were found technically important [1, 2]. Due to lack of boundary grains in their structures these type of materials have some advantages in comparison with crystalline alloys of the same composition. Amorphous alloy ribbons have been studied from different aspects such as magnetic properties, crystalline structure, mechanical properties and crystalline procedure by different tools as X-ray diffraction (XRD), differential scanning calorimetry (DSC), Mössbauer spectrometry, Hall and electrical resistivity measurements, etc. [4, 5]. One characteristic structural feature of amorphous alloys is their short-range order which is thermodynamically metastable [4]. Because these alloys become brittle upon annealing, which causes serious difficulties in handling process and material volume characteristics, many researches try to improve MGs properties by different operations including annealing of the precursor alloy in metastable state [6].

MGs are obtained by rapid solidification from a melt and they evolve through changes of the chemical and topological short-range ordering [5]. Their structure depends on the quenching rates used to produce the alloy. Nasu and Gonser [7] have investigated the ribbon of Metglass 2826 ($Fe_{40}Ni_{40}P_{14}B_6$) produced by a single roller quenching technique. They obtained Mössbauer spectra simultaneously in transmission geometry by measuring γ-rays and in scattering geometry by measuring conversion electrons. Their results obviously show that different magnetic domain structures can simultaneously exist in the bulk and at the surfaces.

Ok and Morrish [8] investigated transformation from as-quenched amorphous to crystalline state in a $Fe_{82}B_{12}Si_6$ metallic glass using both transmission Mössbauer spectrometry and scattering Mossbauer spectroscopy. They have found that the surface crystallization on the wheel (dull) side precedes the bulk crystallization. Similar results were found by these authors also for $Fe_{75.4}B_{14.4}Si_{10.4}$ MG [9]. Nevertheless, as it was shown in [10, 11], the two surfaces of Fe-Nb-B ribbons exhibit different properties due to provoked crystallization in a very thin layer at the wheel side surface. The obtained parameters of coercive fields are different for the wheel (dull) and air (shiny) sides [10, 11]. Also several studies have focused on the $Fe_{78}Si_9B_{13}$ MGs [12, 13].

The above mentioned points motivated us to consider the same system prepared under different production velocity conditions. The previous studies did not explore these effects upon magnetic and structural properties of $Fe_{78}Si_9B_{13}$ amorphous ribbons by Mössbauer spectrometry. One of the aims of the present work is to investigate correlation between the

production velocity and magnetic anisotropy in $Fe_{78}Si_9B_{13}$ MGs and to obtain the details of spin texture [1, 4, 14].

2. Experimental details

Iron-based $Fe_{78}Si_9B_{13}$ MG was fabricated by a melt spinning method in argon atmosphere in a form of ribbons using various tangential disk velocities namely 15, 20, 25, 30, 35, and 40 m/s. This study analyzes the effect of disk velocity through measurements of the samples thickness by a micrometer with the accuracy of 0.001 mm.

Structural properties of the samples were checked by X-ray diffraction using Burker D8 Discover diffractometer employing filtered Cu-K_α radiation. Mössbauer spectra were collected at room temperature in transmission geometry using a conventional constant-acceleration spectrometer equipped with a ^{57}Co γ-ray source in a rhodium matrix.

Mössbauer spectra were analyzed by least-square fitting procedure using the NORMOS fitting software [3]. The spectra were evaluated by Lorentzian line sextets employing distributions of hyperfine magnetic fields P(B). Magnetic anisotropy of ^{57}Fe resonant atoms was characterized by measuring relative ratios of the 2nd and the 5th lines of the sextets that are determined by the angle θ between the directions of the net magnetization and γ-rays.

Surface features of the ribbon prepared with the velocity of 15 m/s were checked at the wheel side by the method of Conversion Electron Mössbauer Spectrometry (CEMS). This method provides information by recording conversion electrons of all energies emitted from scanning depths down to ~ 200 nm. Velocity calibration was performed by an α-Fe foil.

3. Results and discussion

3.1 Thickness of the ribbons

The effect of quenching wheel velocity upon the thickness of the produced MG ribbons is illustrated in Fig. 1. The thickness decreases drastically as the wheel velocity increases. The sample's thickness obtained at the maximum velocity is almost 3 times smaller than that at the minimum one. The error bars associated with the determination of the ribbons' thicknesses are comparable with the size of the symbols used in Fig. 1.

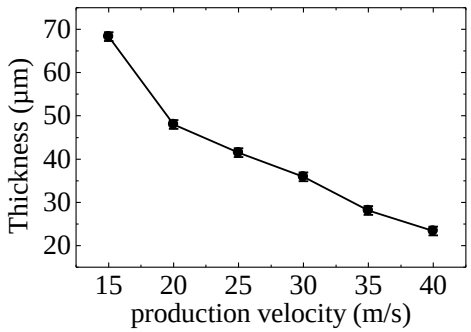

Fig. 1: Thickness of the MG ribbons plotted against velocity of the quenching wheel.

3.2 XRD measurements

Because of lack of any periodical structural arrangement, amorphous materials exhibit broad XRD patterns since in these materials X-rays are scattered in many directions that leads to wide bumps distributed over a wide range of 2θ values instead of high intensity narrow peak reflections that are characteristic for well ordered crystalline structures. XRD patterns obtained for the lowest and the highest velocity, namely 15 and 40 m/s, respectively, are illustrated in Fig. 2. Some signs of narrow reflections are seen only at the wheel side of the

sample produced with the lowest velocity (15 m/s). They are positioned at the Bragg angles of $2\theta = 44.5$, 65, 82.5 and 99^{o}. According to the corresponding lattice parameters we assume that they belong to bcc α-Fe and Fe_3Si nanocrystals. Since only this side of the investigated samples contributes to the diffracted intensity by the above mentioned peaks these results suggest that only one surface is partially crystallized whereas bulk parts and the remaining surfaces are fully amorphous as documented by broad peaks at $2\theta = 45^{o}$ in all patterns.

The presence of Fe_3Si phase is expected because all Si and B atoms are surrounded by only Fe atoms and the correlations Si–Si, Si–B, and B–B are likely bridged by them. Since the Fe–Si bonding is stronger than the Fe–B one a DO_3-type Fe,Si solid-solution-like structure should nucleate more easily from the amorphous matrix [15].

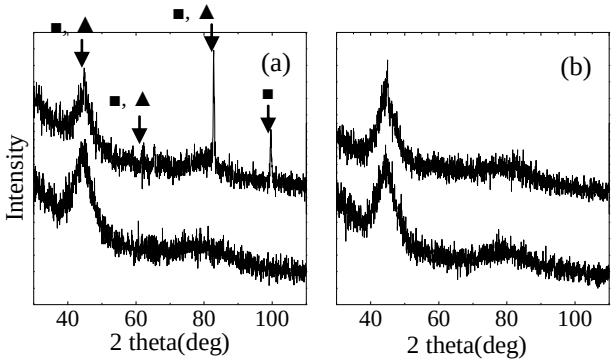

Fig. 2: XRD patterns taken from (a) the wheel and (b) air side of the $Fe_{78}Si_9B_{13}$ ribbons with the lowest (15m/s) and the highest (40m/s) production velocity. The narrow reflections are assigned to (■) α-Fe and (▲) F_3Si nanocrystals.

3.3 Mössbauer spectrometry

Structural disorder in amorphous materials leads to an existence of a large number of nonequivalent atomic sites. Consequently, physical parameters such as hyperfine interactions, magnetic moments, and exchange interactions have to be analyzed in terms of their continuous distribution. In this way, we can obtain a view into the amorphous structure and the influence of structural disorder upon the physical properties, too [16].

Mössbauer spectra obtained from transmission geometry experiments performed at room temperature are shown in Fig. 3 together with the corresponding P(B) distributions. The spectra exhibit well separated six broad absorption lines which are characteristic for fully amorphous ferromagnetic material. They we were evaluated using hyperfine magnetic field distributions P(B) (see Fig. 3b). It is noteworthy, that in the analysis of the Mössbauer spectra we took into consideration also the results of XRD measurements. They suggest full amorphicity of the investigated ribbons with one exception that is discussed below.

In the absence of any stresses in the specimen, atomic spins are expected to remain within the ribbon plane due to shape anisotropy thus making the Mössbauer line intensity ratio $A_{23} = 4$. On the other hand, for completely random spin alignment $A_{23} = 2$. Thus, change in A_{23} can be used to monitor spin texture in the specimens [1, 4].

Fig. 3 depicts Mössbauer spectra of all investigated samples in the as-quenched state. Each spectrum exhibits broad sextuplet lines typical for amorphous ferromagnet so they were fitted by distributions of Zeeman sextets. The obtained Mössbauer spectra indicate that the studied as-cast ribbons are soft magnetic materials. According to Fig. 3a the line width generally increases from the inside pair (3,4) to the outside pair (1,6) of absorption lines in all samples. The increasing line width indicates the importance of field fluctuations which tend to dominate in the outer lines [2]. The spectra are smooth, i.e. no structures like shoulders are present within the lines themselves. The spectra also exhibit line width and line intensity

asymmetries which are also typical for metallic glasses. Relatively large line widths are a consequence of the distribution of hyperfine interactions. In addition, as can be seen from Fig. 3, the intensities of the second and fifth lines systematically decrease towards higher velocity indicating that spin orientations tend to be out of the sample plane. Nevertheless, a deviation from this pattern is observed in the 15 m/s sample.

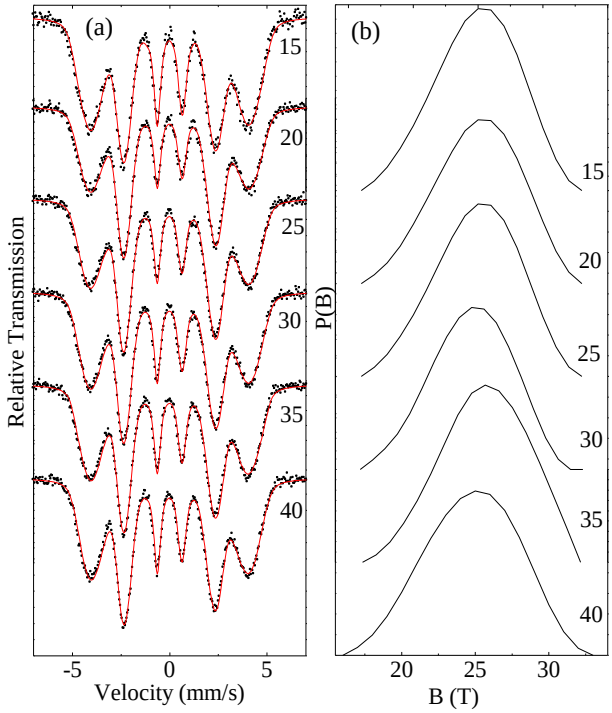

Fig. 3: Room temperature transmission ^{57}Fe Mössbauer spectra (a) and corresponding hyperfine magnetic field distributions P(B) (b) of the as-quenched $Fe_{78}Si_9B_{13}$ MGs prepared with the indicated velocities (m/s) of the quenching wheel.

Variation of average values of the hyperfine magnetic fields and A_{23} as a function of the production velocity are illustrated in Fig. 4. The magnetic moments are widely spread in the as-cast $Fe_{78}Si_9B_{13}$ amorphous ribbons. Consequently, a complex anisotropy distribution caused by the internal stresses induced during the quenching process is observed in Fig. 4a by notable deviations in A_{23} parameters namely at the low production velocity region.

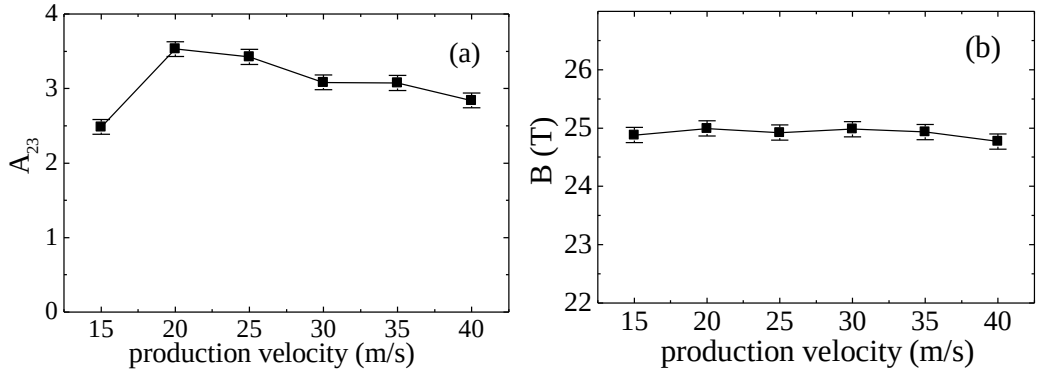

Fig. 4: Plot of A_{23} (a) and the average hyperfine magnetic field (b) against the production velocity for as quenched samples.

On the other hand, the average hyperfine magnetic fields plotted in Fig. 4b are stable over the entire range of production velocities. This means that the average hyperfine magnetic field does not depend upon the thickness of the ribbons though orientation of the particular magnetic moments is considerably affected.

Because transmission Mössbauer spectra have not revealed any traces of crystalline phases in the bulk of the ribbon, we have performed CEMS which scans the surface regions. As an example, CEMS spectrum taken from the wheel side of the as-quenched $Fe_{78}Si_9B_{13}$ ribbon prepared with the velocity of 15 m/s is shown in Fig. 5 together with the corresponding P(B) distribution. As it can be seen this sample exhibits no apparent signs of narrow lines which could indicate presence of crystallites as follows from the XRD results. This is possibly due to very low crystalline content and the expected Mössbauer spectral lines are completely overlapped with a broad sextuplet from the amorphous matrix.

Since the wheel side is in direct contact with the rotating wheel, quenching rate of the solidification process is faster than that in a bulk [17]. Consequently, we can expect some differences between surface and bulk hyperfine parameters. The average ^{57}Fe hyperfine magnetic field in the bulk as-quenched state of the 15 m/s sample is 24.88±0.13 T, while that of the corresponding ribbon surface is 24.84±0.13 T. So we can conclude that the local iron atoms environments are practically unchanged.

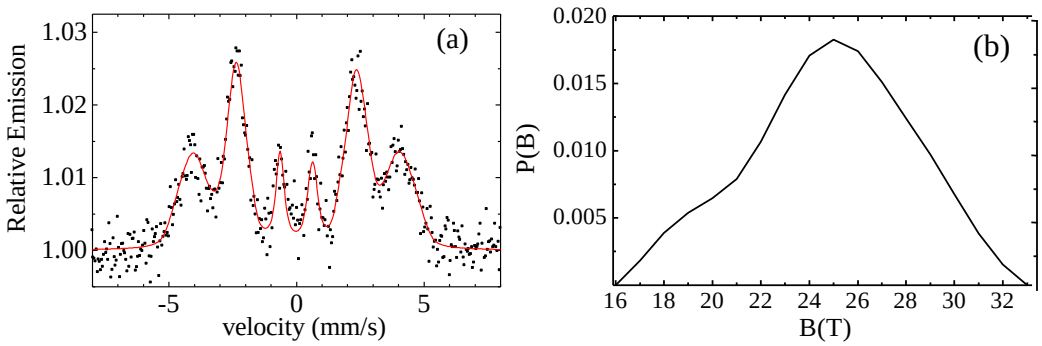

Fig. 5: CEMS spectrum taken from the wheel side (a) and corresponding hyperfine magnetic field distribution P(B) (b) of the as-quenched $Fe_{78}Si_9B_{13}$ MG prepared with 15 m/s.

Nevertheless, as far as orientation of the magnetic moments positioned in bulk and on the surface of the ribbons is concerned, the bulk shows close-to-random arrangement of the moments (A_{23} = 2.48) whereas the surface is highly textured (A_{23} = 3.83). Surface magnetic moments are oriented close to the ribbon plane, i.e. perpendicular to the Mössbauer γ-ray direction.

4. Conclusion

We have studied the $Fe_{78}Si_9B_{13}$ using transmission and CEMS Mössbauer spectrometry and XRD. Varying the quenching wheel velocity, ribbons with different thicknesses were produced. XRD measurements as well ^{57}Fe Mössbauer spectrometry studies indicated amorphous nature of the produced ribbons with one exception. At the wheel side of the lowest velocity namely 15 m/s, presence of small amounts of Fe_3Si crystallites was unveiled by XRD. Mössbauer experiments performed in transmission geometry as well as using conversion electrons emitted from near surface regions have not confirmed these findings most probably because of the detection limits.

A correlation of magnetic anisotropy with changing production velocity was found using relative areas of the 2nd and the 5th lines of the Mössbauer spectra. Nevertheless,

despite variations in the latter, the average hyperfine magnetic fields are almost equal within the experimental error range. Thus, the local magnetic fields in the as-quenched state are independent on the production velocity.

Despite variations in the A_{23}(relative areas of the 2nd and the 5th lines), the average hyperfine magnetic fields are almost equal within the experimental error range, Thus they are independent on the production velocity.

Acknowledgement

This work was supported by the grants GACR 14-12449S, and VEGA 1/0182/16. NA acknowledges financial support from the Ministry of Science, Research and Technology of the Islamic Republic of Iran during her stay at the Slovak University of Technology in Bratislava.

References:

[1] E. Kuzmann, S. Stichleutner, A Sápi, L. K. Varga, K. Havancsák, V. Skuratov, Z. Homonnay, A. Vértes, *Hyperfine Interactions*, **207**, 73 (2012).
[2] A. K. Bhatnagar, *Hyperfine Interactions*, **25**, 637 (1985).
[3] R. A. Brand: NORMOS programs, Universitaet Duisburg, Germany (1987).
[4] X. Li, K. Zhang, C. Wang, W. Han, G. Wang, *J. Mater. Sci. Technol.*, **23,** 253(2007).
[5] E. Jakubczyk: *Materials Science-Poland*, **24**, 1027 (2006).
[6] Y. H. Chang, C. H. Hsu, H. L. Chu, C. W. Chang, W. S. Chan, C. Y. Lee; C. S. Yao, Y. L. He, *Int. J. Electrical, Computer, Energetic, Electronic and Comm. Eng.*, **5**, 1160 (2011).
[7] S. Nasu, U. Gonser, *J. de Phys.*, **41**, C8-689 (1980).
[8] H. N. Ok, A. H. Morrish, *Phys. Rev. B*, **22**, 3471 (1980).
[9] H. N. Ok, A. H. Morrish, *J. Phys. F*, **11**, 1495 (1981).
[10] L. Kraus, O. Zivotsky, L. Postava, P. Svec and D. Janickovic, *IEEE Trans Magn.*, **44**, 3875 (2008).
[11] M.S. Leu and T.S. Chin: In: *MRS Proceedings*, M. Coey, L.H. Lewis, B-M. Ma, T. Schrefl, L. Schultz, J. Fidler, V.G. Harris, R. Hasegawa, A. Inoue, M.E. McHenry (ed.), Cambridge, England, 557 (1999).
[12] E. Jakubczyk, A. Krajczyk, M. Jakubczyk, *Journal of Physics*, **79**, 12008 (2007).
[13] J. M. Cadogan, S. J. Campbell, J. Jing, C. P. Foley, P. Kater, Y. W. Mai, *Hyperfine Interact*, **226**, 7 (2014).
[14] S. N. Kane, A. Gupta, L. K. Varga, *J. Magn. Magn. Mat.*, **254–255**, 501 (2003).
[15] J. Qin, T. Gu, L. Yang, X. Bian, *Appl. Phys. Lett.*, **90**, 201909-2 (2007) .
[16] C. L. Chien, G. Xiao, K. M. Unruh, *Phys. Rev. B*, **32**, 5582 (1985).
[17] M. S. Rogalski, I. Bibicu, *phys. status solidi b*, **195**, 531 (1996).